Vacancy ordering phase transition in $ZrBe_2(H/D)_x$: NMR and electronic structure study

Vikram D. Kodibagkar,[1,*] Peter A. Fedders,[1] Caleb D. Browning,[1] Robert C. Bowman, Jr.,[2] Natalie L. Adolphi,[3] and Mark S. Conradi[1]

[1]*Department of Physics, Washington University, St. Louis, Missouri 63130-4899*

[2]*Jet Propulsion Laboratory, California Institute of Technology, Pasadena, California 91109-8099*

[3]*Knox College, Galesburg, Illinois 61401*

(Received 19 July 2002; published 22 January 2003; corrected 30 January 2003)

The layered intermetallic compound $ZrBe_2(H/D)_x$ ($x \simeq 1.5$) was studied using deuterium and beryllium NMR. A temperature-induced structural transition in the deuteride reported earlier is further investigated here using ^{9}Be NMR, which reveals the transition in both the hydride and deuteride at 200 and 235 K, respectively. Above the transition temperature a single pair of quadrupolar satellites is present. Each quadrupolar satellite splits into two resonances below the transition temperature, implying the existence of two different classes of Be sites. The temperature dependence of the satellite frequencies and the appearance of two-phase coexistence spectra show the transition to be first order. Be-D spin-echo double resonance (SEDOR) experiments were performed to identify the two sites; SEDOR demonstrates that the D environments of the two classes of Be sites are similar. Electronic structure calculations show the binding energy of H decreases gradually for x greater than 1.38. The calculations allow a vacancy ordered structure to be proposed.

DOI: 10.1103/PhysRevB.67.045107 PACS number(s): 76.60−k, 75.20.−g

I. INTRODUCTION

The intermetallic compound $ZrBe_2$ crystallizes in a hexagonal AlB_2-type structure[1] consisting of alternate layers of zirconium (Zr) and beryllium (Be) atoms. The Zr atom and two Be atoms reside at (0,0,0), $(\frac{1}{3},\frac{1}{3},\frac{1}{2})$, and $(\frac{2}{3},\frac{2}{3},\frac{1}{2})$, respectively in the unit cell with lattice parameters $a = 3.820$ Å and $c = 3.240$ Å.[1] This compound reacts with hydrogen at room temperature and one atmosphere of hydrogen pressure, spontaneously and exothermally, to absorb up to 1.5 hydrogen (H) or deuterium (D) atoms per unit cell.[2] Neutron diffraction[3] indicates that the D atoms reside in the hexagonal Zr planes directly above and below each Be atom (see Fig. 1), at the centers of triangles formed by Zr atoms, i.e., at the $2c$ sites, $(\frac{1}{3},\frac{1}{3},0)$ and $(\frac{2}{3},\frac{2}{3},0)$. Thus, theoretical full occupation of the available H sites in $ZrBe_2H_x$ corresponds to two H atoms per formula unit ($x=2$), but forming hydrides beyond $x=1.5$ requires extremely large H_2 pressure and the absorbed hydrogen is lost upon return to one atmosphere.[2] Forming deuterides with $x=1.5$ results in a 7.3% expansion along the **c** axis and a 2.7% contraction along the **a** axes (with no change in crystal symmetry), resulting in the lattice parameters $a=3.714$ Å and $c=3.470$ Å.[3] The considerable expansion of the **c** axis upon forming hydrides indicates an effective Be-H (or Be-D) repulsion while the **a**-axis shrinkage indicates Zr-H attraction. Westlake[4] suggested that the H (D) atoms may occupy either (but not both) of the slightly off-plane $4h$ sites. These sites occur in pairs, only 0.064 Å above and below each $2c$ site (i.e., displaced along the **c** axis). Fast local motion between the $4h$ sites at room temperature may average the apparent position to $2c$, as reported by neutron diffraction.[3]

The abundance of vacant hydrogen sites facilitates rapid site-to-site diffusion; the H atoms are quite mobile with about 10^8 hops/sec at room temperature between neighboring sites (presumably $2c$) in the hydride.[5] The intervening layer of Be atoms blocks H atoms from hopping between planes so that H diffusion is strictly two-dimensional, according to NMR studies of $ZrBe_2H_{1.4}$. The logarithmic frequency dependence of the spin lattice relaxation rate T_1^{-1} in both static field[6] and field-cycling measurements[7] clearly fit a two-dimensional (2D) model. Pulse field-gradient measurements of diffusion[7] report the rate of diffusion along the gradient axis, which is randomly oriented relative to each powder particle. The resulting nonexponential decay of the spin-echo signal amplitude as a function of squared gradient amplitude matches the dependence expected for two-dimensional diffusion.

A powder neutron diffraction study of $ZrBe_2D_{1.5}$ reported a temperature-induced structural change[8] below 250 K. Weak superlattice peaks were observed upon cooling. A model with occupation of the $4h$ sites resulted in improved Rietveld refinements at 12 K. The study suggested a disorder-to-order like change in the deuterium site occupancy from $2c$ to $4h$ on cooling, but did not attempt to fit the new peaks to a model of ordered vacancies. The same study also noted that powder x-ray diffraction data showed no line splittings or additional reflections on decreasing the temperature in the range 120–600 K for $ZrBe_2$ and $ZrBe_2D_{1.5}$, suggesting that the structural change primarily affects the D positions (deuterium atoms contribute negligibly to x-ray diffraction). A deuterium NMR study conducted by our group[9] finds a rapid increase in the ^{2}D transverse spin-relaxation rate T_2^{-1} below 240 K in the deuteride. This, along with the neutron diffraction results,[8] indicates a stronger effect than just a small change in D-atom positions from $2c$ sites to the nearby $4h$ sites. We proposed that the transition involves ordering of the D vacancies (25% at $x=1.5$). The observed increase in T_2^{-1} is then an expected result of the decreased D-atom mobility that would occur in a vacancy-ordered configuration.

We note that previous hydrogen NMR studies of $ZrBe_2H_{1.4}$ reported no evidence of a phase transition in the

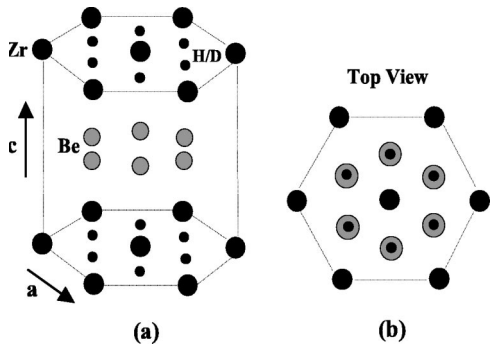

FIG. 1. Crystal structure of $ZrBe_2(H/D)_x$. (a) Alternate layers of Zr and Be atoms with H or D atoms residing in the Zr plane, directly above and below beryllium atoms. The lattice parameters are $a=3.714$ Å and $c=3.470$ Å at $x=1.5$, where 25% of the H sites are vacant. (b) Looking down the c axis. The H positions and Be projections are at the centers of triangles formed by Zr atoms. In the bare compound $ZrBe_2$, only the lattice parameters are different.

hydride.[5–7] In particular, the T_1 data extending from 115 K to 400 K are well described by a model with a single activation energy.[5] The apparently different phase behaviors of the deuteride and hydride partly motivated this study. Beryllium-9 has nuclear spin 3/2 with 100% abundance and has an NMR frequency close to that of deuterium. As beryllium is present in the hydride, the deuteride, and the bare $ZrBe_2$ as well, ^{9}Be spectroscopy should allow the transition to be better characterized by comparing the three materials.

We report here ^{9}Be spectra for $ZrBe_2$, $ZrBe_2H_{1.4}$, and $ZrBe_2D_{1.4}$. In the cases of $ZrBe_2H_{1.4}$ and $ZrBe_2D_{1.4}$, spectra were obtained at many temperatures. For these, magnetic alignment of the powder samples substantially simplified the interpretation of the NMR spectra. Spin-echo double resonance (SEDOR) experiments between ^{9}Be and ^{2}D were performed in an attempt to identify the ^{9}Be resonances in the low-temperature phase.

II. EXPERIMENTAL DETAILS

The $ZrBe_2H_x$ and $ZrBe_2D_x$ samples were prepared by A. J. Maeland. The preparation procedures of the powder samples have been reported previously.[2] A part of the $ZrBe_2H_x$ sample was changed to $ZrBe_2$ by heating it at 700 °C under vacuum. Measurements were made in superconducting magnets at fields of 4.4 and 8.0 T, using a computer-controlled home-built pulsed NMR spectrometer and a Chemagnetics CMX360 spectrometer. The data acquisition and analysis on the home-built spectrometer were performed using a program FIDO written by our group in LabWindows CVI (C for Virtual Instrumentation) programming language. Spectra were obtained using the $(\pi/2)_x$-τ-$(\pi/2)_y$ echo sequence by Fourier transforming short-τ echoes. For ^{9}Be NMR studies a 1000 W transmitter was used as narrow radio frequency (rf) pulses (2–4 μs) were required to excite the entire broad resonance. The temperature at the sample was varied using flowing N_2 gas or air controlled by an electronic thermostat. The temperatures were steady to within ± 0.5 K and were measured using a type-T (copper-constantan) thermocouple with a room temperature reference.

The SEDOR experiment[11,12] consists of a spin-echo pulse sequence on the nucleus of interest (*observed* nucleus, here ^{9}Be) with an additional π pulse on another nucleus (*unobserved* nucleus, here ^{2}D) that interacts with ^{9}Be via the dipole-dipole interaction. The π pulse on ^{2}D approximately coincides with the refocusing pulse of the spin-echo sequence on ^{9}Be. We denote the time between the two pulses on ^{9}Be as τ and the π pulse on ^{2}D is applied at a time t after the first pulse on ^{9}Be. The time t is slightly larger than τ allowing the ^{9}Be and ^{2}D pulses to be generated sequentially in a single rf transmitter. The spin-echo amplitudes of ^{9}Be with (S_w) and without ($S_{w/o}$) a π pulse on ^{2}D are obtained as a function of $4\tau-2t$ (the ^{9}Be-^{2}D interaction is effective over a time $2[\tau-(t-\tau)]=4\tau-2t$). The value of $t-\tau$ was held fixed as τ was varied. The decay curve $S_w/S_{w/o}$ as a function of $4\tau-2t$ is ideally the ^{9}Be free-induction decay (FID) that would occur if the only spin interactions were ^{9}Be-^{2}D dipolar. Hence, the decay rate is a measure of the dipolar interaction between ^{9}Be and ^{2}D. For our SEDOR experiments, a double resonance probe was constructed for ^{9}Be and ^{2}D frequencies at 8.0 T (47.87 MHz and 52.29 MHz, respectively). The design[10] is based on symmetric and antisymmetric modes of two coupled, identical LC circuits, with the frequency spacing of the two modes determined by a coupling capacitor. This approach is particularly suitable when the two frequencies are nearly equal, as in our case. Separate frequency synthesizers were used for the two frequencies with a *p-i-n* diode switch to select between the two; otherwise the rf pulse generation and high-power amplification were common to both frequencies.

Calculations of the electronic energy and structure were performed with SIESTA (Spanish Initiative for Electronic Simulations with Thousands of Atoms) using a supercell containing 16 Be atoms, 8 Zr atoms, and from 0 to 16 H atoms. With this supercell we found it necessary to use 27 $(3\times3\times3)$ k points in the Brillouin zone in order to get energy differences between supercells that were reliable to better than 0.01 eV. We used 5 orbitals each for the Be and H atoms but found it necessary to use 19 orbitals ($4s$, $4p^3$, $4d^5$, $5s$, and a set of excited spd orbitals) for the Zr atoms. The supercell was relaxed with respect to size and shape in the stochiometric limits of $x=0$ and $x=2$; a linear interpolation was used in between. As expected, the lattice parameters c increased and a decreased with increasing x,[1–3] but the lattice parameters differed from the experimental values by several percent. Crucially, energy *differences* using the experimental lattice parameters differed only minimally from the energy differences quoted.

III. RESULTS AND DISCUSSION

A. Beryllium spectra

Figure 2 shows ^{9}Be spectra for powders of $ZrBe_2$, $ZrBe_2H_{1.4}$ and $ZrBe_2D_{1.4}$ at 270 K in a field of 8.0 T. The $ZrBe_2$ sample was obtained by removing hydrogen from another $ZrBe_2H_{1.4}$ sample. The $ZrBe_2$ spectrum shows the ex-

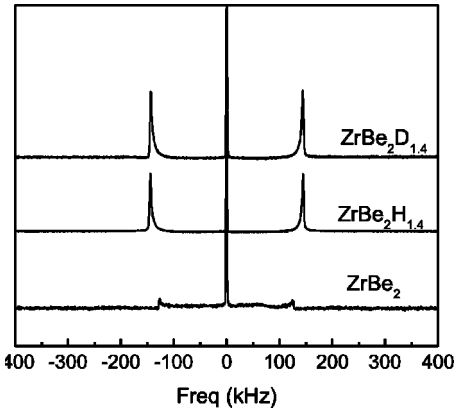

FIG. 2. ^{9}Be spectra of $ZrBe_2$, $ZrBe_2H_{1.4}$, and $ZrBe_2D_{1.4}$ at 270 K. The vertical scale is normalized to approximately the same central transition intensity. For $ZrBe_2H_{1.4}$ and $ZrBe_2D_{1.4}$ sharp satellites occur because of magnetic alignment of the powder particles. For $ZrBe_2$, the satellite intensity is spread over the powder pattern, indicating that magnetic alignment does not occur.

pected broad powder pattern with a cusp-to-cusp splitting of 250 kHz for the quadrupolar satellites ($m=-\frac{3}{2}\leftrightarrow-\frac{1}{2}$ and $+\frac{3}{2}\leftrightarrow+\frac{1}{2}$) and a narrow central transition ($m=-\frac{1}{2}\leftrightarrow\frac{1}{2}$). The hydride and deuteride show remarkably sharp satellites with a satellite-to-satellite splitting of 287 kHz. Although the samples are powders, the spectra do not show the characteristic powder pattern. Instead sharp satellites appear, as would occur for a single crystal. From the spectra we can conclude that both the hydride and deuteride exhibit strong preferential alignment of the powder particles in the magnetic field while the bare $ZrBe_2$ does not (the bare compound may have become lightly sintered during hydrogen removal at 700 °C). Comparison of the spectrum of $ZrBe_2D_{1.56}$ frozen in wax at zero field (effectively an unaligned powder) with that of a sample magnetically aligned in 8.0 T shows that the sharp lines of the aligned sample's spectrum occur at the same frequencies as the cusps (90° features) of the unaligned powder. By symmetry, the unique axis of the single electric field gradient (EFG) tensor describing the ^{9}Be in the regime of fast deuterium motion must be the crystalline c axis. Thus, the particles align with their c axes perpendicular to the applied magnetic field. The high degree of alignment demonstrates that virtually all of the powder particles are single crystallites. The alignment is due to magnetic susceptibility anisotropy. For this study we note that the magnetic alignment substantially simplifies the interpretation of the spectra.

Spectra of ^{9}Be were obtained for samples of $ZrBe_2D_{1.4}$ and $ZrBe_2H_{1.4}$ from 120 to 300 K; representative spectra are presented in Figs. 3 and 4. For the deuteride, as the temperature is decreased, the spectrum changes very little until the temperature reaches 235 K. Below 235 K, each satellite splits into two, with satellite-to-satellite splittings of 225 kHz and 350 kHz, respectively. This is consistent with a phase transition at this temperature, as suggested in a previous report[9] based on rapid changes in ^{2}D T_2^{-1} and by the appearance of superlattice peaks in the neutron diffraction patterns.[8] The NMR spectra imply the existence of 2 separate classes of Be sites below the transition temperature T_c. These are

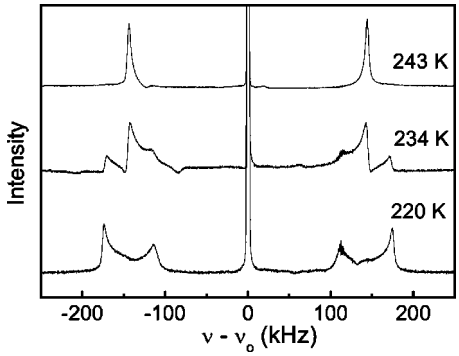

FIG. 3. ^{9}Be spectra of $ZrBe_2D_{1.4}$ as a function of temperature. The single pair of satellites for $T>235$ K splits into two pairs below 235 K. A mixed-phase spectrum occurs at temperatures near 235 K, showing the first-order nature of the transition. The central transition is narrow so its amplitude is off-scale.

labeled as I and O sites (corresponding to inner and outer satellites, respectively). As the temperature is decreased further, the spectrum changes very little except for slight additional broadening.

The ^{9}Be spectra of Fig. 4 clearly show that a similar transition occurs in the hydride, but at a lower temperature of about 200 K. In an earlier report,[9] we speculated that the hydride may not undergo a transition, based on the absence of any changes in temperature dependence of the proton NMR T_1 and $T_{1\rho}$ data.[5,6] However, at the 200 K transition temperature, the proton T_1 is becoming limited by the Korringa[14] (conduction electron) contribution and so is less sensitive to hydrogen motion. Changes in the slope of the proton $T_{1\rho}$ data as a function of temperature should be evident, but do not appear in the experimental results.[5]

In Fig. 5, the quadrupolar splittings ν_Q between the higher and lower frequency satellites are plotted as a function of temperature for the hydride (solid symbols) and the deuteride (open symbols). The single value of ν_Q seen above T_c changes to two ν_Q values below T_c (corresponding to two pairs of satellites). All three pairs of satellites are present in a small interval centered upon T_c, showing the coexistence of the two phases. The discontinuous changes of ν_Q occurring near T_c along with two-phase coexistence demonstrate that the transitions are first order. The neutron diffraction study[8]

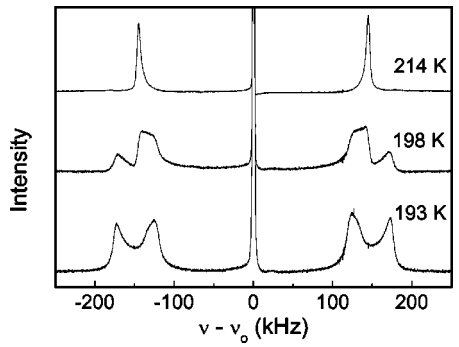

FIG. 4. ^{9}Be spectra of $ZrBe_2H_{1.4}$ as a function of temperature. The behavior is similar to the deuteride spectra of Fig. 3, but with a transition temperature near 200 K.

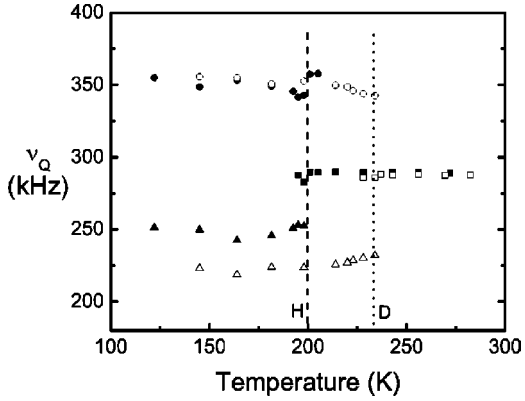

FIG. 5. ν_Q (the satellite to satellite splitting) from ^{9}Be spectra of $ZrBe_2H_{1.4}$ (solid symbols) and $ZrBe_2D_{1.4}$ (open symbols) as a function of temperature. The circles and triangles represent the outer and inner satellites, respectively, in the low-temperature phase. The squares represent the single splitting in the high-temperature phase. Two-phase coexistence is observed for a narrow range in temperature for both the hydride and the deuteride. The dashed and dotted lines represent the transition temperatures for the hydride and deuteride, as labeled.

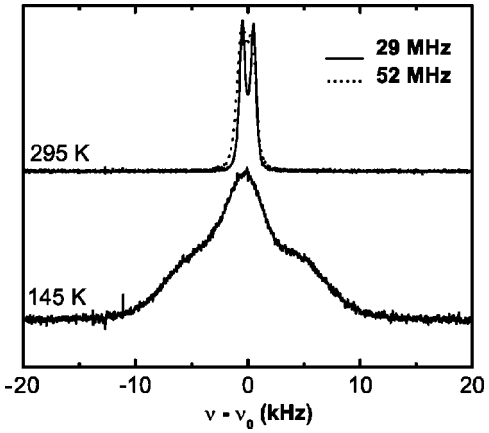

FIG. 6. Deuterium NMR spectra well above (295 K) and below (145 K) the transition temperature for $ZrBe_2D_{1.4}$ at 29 MHz. Also shown, as dotted curve, spectrum at 295 K obtained at 52 MHz.

reported a continuous increase in superlattice peak intensity with temperature decreasing over a 50 K window. We believe the diffraction intensity data do not show the transition to be higher order, but show the effect of the two-phase coexistence.

Above T_c, the hydride and deuteride have almost equal ν_Q (see Fig. 5), with the value reflecting a motional average as the vacancies diffuse rapidly through the structure. Below T_c, the outer satellite ν_Q values are essentially the same for the hydride and deuteride, while there is a substantial isotopic difference in the inner ^{9}Be ν_Q values. This difference is not understood. We note that in a simple picture, the inner and outer ν_Q must average (with concentration dependent weighting factors) to the high-temperature ν_Q value. Thus it is unexpected that only the inner ν_Q is different in the hydride and deuteride, given that both materials have nominally equal concentrations, $x=1.4$.

The line shapes of the quadrupolar satellites of both the hydride and deuteride materials are distinctive in the low-temperature phase (Figs. 3 and 4). For example, in Fig. 4 the outer edges (at ± 125 and ± 175 kHz) are comparatively sharp, with gradual intensity variation in between. This suggests that some of the linewidth in the low-temperature phase is due to angular variation (as in a two-dimensional powder pattern).[12,13]

The ^{9}Be central transition of $ZrBe_2D_{1.4}$ in the low-temperature phase under magic-angle spinning conditions (not shown) is well-described by the sum of two components with relative widths of 2.44:1. This is the expected result of second-order broadening, proportional to the square of ν_Q (ν_Q values from Fig. 5 in ratio 1.56:1). These results support the picture of two separate quadrupolar satellite pairs.

B. Deuterium spectra

In light of the fact that the powder particles align in the magnetic field, the deuterium spectra reported earlier[9] deserve another look. Figure 6 shows deuterium NMR spectra for $ZrBe_2D_{1.4}$ at 295 K ($T \gg T_c$) and 145 K ($T \ll T_c$). The spectrum at 295 K is shown at two different frequencies (29 and 52 MHz) while the other spectrum was obtained at 29 MHz. At 295 K, motional averaging yields a quadrupolar doublet with a small splitting (~ 1 kHz), independent of the NMR field and frequency, as expected for a quadrupolar interaction. The splitting results from a small but nonzero EFG average over all occupied sites. It is surprising that the average EFG at the D sites is so small, as there is no symmetry requirement for the EFG to average to zero over the sites of a hexagonal lattice. The sharpness of the doublet is due to the alignment effect (as observed in the ^{9}Be spectra). At and below 145 K, a temperature-independent spectrum occurs, showing that motional averaging has ceased (no motions on the NMR time scale, of order 10^{-3} s). The low-temperature spectrum arises from a superposition of quadrupolar doublets from sites (with a broad distribution of individual EFG's) each convoluted with a Gaussian shape from D-D and Be-D dipolar broadening. These individual doublets are not powder doublets due to the alignment exhibited by the powder particles.

In the ideal ($x=2$) structure represented in Fig. 1, all of the D sites are energetically identical and have identical EFG tensors (both in tensor principal values and directions). This statement is equally true for the in-plane $2c$ sites and the slightly displaced $4h$ sites. In the ideal structure, motion of the D atoms would not modulate the EFG and there would be no increase in ^{2}D linewidth at low temperatures where motion has ceased on the NMR times cale, except for dipolar broadening (estimated to be only 2 kHz.[9]) Thus, the substantial broadening observed in Fig. 6 in going from room temperature to 145 K demonstrates that there are substantial EFG's that differ from site to site. That is, displacements of the atoms (away from their long-range averaged locations) surrounding a vacant deuterium site (recall 1 in 4 sites is vacant at $x=1.5$) are responsible for the bulk of the EFG's evident in Fig. 6 at 145 K.

The EFG at an individual D-atom site need not be uniaxially symmetric with the symmetry axis along the crystal **c**

TABLE I. ^{2}D contribution to $\langle \Delta\omega_d^2 \rangle_{\mathrm{Be}}$ in the undistorted structure. The two nearest neighbors have the maximum contribution.

Shell	No. of atoms (n)	Distance r(Å)	$\Sigma_i \left(\frac{1}{r^6}\right)(3\cos^2\theta_i - 1)^2$ (10^{-2} Å^{-6})	$\langle \Delta\omega_d^2 \rangle_{\mathrm{Be}}$ contribution (%)
1	2	1.735	7.3272	89.5
2	6	2.758	0.5716	7.0
3	12	4.099	0.2030	2.5
4	6	4.626	0.0560	0.6
5	2	5.206	0.0093	0.1

axis, unlike the EFG averaged over all sites. We recall that the **c** axes of the crystallites are magnetically aligned to be perpendicular to the *B* field, but this does not mean the **c** axes are all parallel. Thus some of the broadening evident in Fig. 6 at 145 K may be due to the incomplete style of alignment of the powder samples. The same issue may be present in ^{9}Be spectra below T_c. There the EFG tensors need not be uniaxially symmetric about the **c** axis because of the distortions near each of the H or D vacancy; some of the increased linewidth below T_c may be due to a distribution of angles between the tensor elements and the applied magnetic field.

C. SEDOR results

As the material undergoes vacancy ordering below T_c, two kinds of Be atoms become distinguishable in Figs. 3 and 4. Some Be atoms have two H/D neighbors in the $\pm\mathbf{c}$ direction (see Fig. 1) and others have one H/D atom and one H/D vacancy near it. Henceforth we shall refer to these two kinds of beryllium sites as type *A* and type *B*, respectively. For $x = 1.5$ H/D concentration, there are equal numbers of sites *A* and *B*. For $x = 1.4$ (as in our sample) we expect *A* and *B* sites in the ratio 2:3, respectively. It is tempting to identify the two pairs of satellites observed below T_c (*I*, inner; *O*, outer) with type *A* and *B* beryllium atoms. In order to test this, SEDOR experiments were performed on $ZrBe_2D_{1.4}$.

First, the deuterium contribution to the static dipolar second moment $\langle \Delta\omega_d^2 \rangle_{\mathrm{Be}}$ of a typical beryllium atom was calculated assuming that all the D sites are filled.[12] The direction of the applied field was taken to be perpendicular to the *c* axis (i.e., in the **ab** plane). In Table I, we list the distances to various ''shells'' of deuterium atoms from a generic beryllium atom, the number of deuteriums in each shell and the dipolar second moment contribution of that shell. The table clearly shows that the largest contribution (89.5%) to $\langle \Delta\omega_d^2 \rangle_{\mathrm{Be}}$ comes from the closest shell although it contains only two deuterium atoms. Naturally, should one of these two atoms be missing, one expects a significant change in $\langle \Delta\omega_d^2 \rangle_{\mathrm{Be}}$. Assuming a 75% occupation of shells 2 and higher, and for the first shell two D atoms present for case *A* and one D atom present for case *B*, the values of $\langle \Delta\omega_d^2 \rangle_{\mathrm{Be}}$ for type *A* and *B* atoms are 1.404×10^7 rad^2/s^2 and 0.758×10^7 rad^2/s^2, respectively. For a Gaussian decay, $\langle \Delta\omega_d^2 \rangle_{\mathrm{Be}}$ is related to the time T_2 for the decay of $S_w/S_{w/o}$ to $1/e$ of its initial value as $T_2 = (\langle \Delta\omega_d^2 \rangle_{\mathrm{Be}}/2)^{-1/2}$. The calculated values of $\langle \Delta\omega_d^2 \rangle_{\mathrm{Be}}$ lead to expected decay times of 377.4 μs and 513.7 μs for type *A* and *B* atoms, respectively. SEDOR experiments (^{9}Be observed, ^{2}D unobserved) performed at temperatures low enough to freeze out D motion are thus expected to show significantly faster decay of the SEDOR curve for type *A* beryllium atoms due to the presence of two deuterium atom nearest neighbors, as opposed to one for type *B*. Thus it should be possible to test whether the two satellites in the low temperature spectrum (*I* and *O*) correspond to Be atoms *A* and *B*.

We performed ^{9}Be-^{2}D SEDOR experiments[12] on $ZrBe_2D_{1.4}$ at 145 K and 104 K. The spectrometer frequency was chosen to be centered between the two lower-frequency satellites *I* and *O* in the beryllium spectrum (47.73 MHz). The sharpness of the satellites and the clean separation from the central transition and higher-frequency satellites allowed us to treat the $\frac{3}{2} \leftrightarrow \frac{1}{2}$ transition as an effective two-level system. Soft $\pi/2$ and π pulses (10 μs and 20 μs) were used to create spin echoes from this transition only. The spin echoes were Fourier-transformed and the two satellites integrated in the frequency spectrum to determine their intensities as functions of $4\tau - 2t$. The data are shown in Fig. 7. The data at 145 K were obtained first and show very little difference in

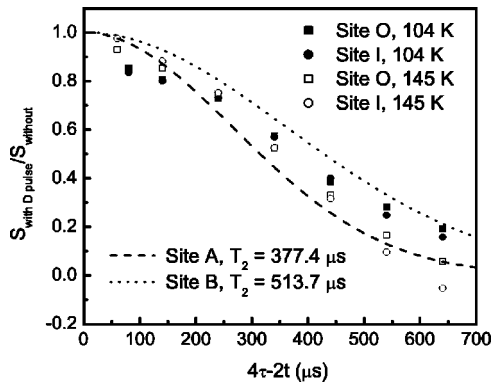

FIG. 7. SEDOR amplitude ratio curves at 145 K and 104 K. Sites *O* and *I* refer to the outer and inner ^{9}Be quadrupolar satellites in the low-temperature phase ($\nu_Q = 350$ kHz and 225 kHz, respectively), on the low-frequency side of the central transition (i.e., $\nu_Q/2$ below the central transition). The data are presented in terms of the time $4\tau - 2t$ over which the ^{9}Be-^{2}D dipolar interactions are effective. The dashed and dotted curves represent the calculated Gaussian decays for *A* and *B* sites, respectively.

the SEDOR decay for the two satellite resonances *I* and *O*. The data indicate that the deuterium environments (populations and distances) of the two classes of Be sites yielding the separate satellite resonances are similar. Because it is possible that residual deuterium motion (vacancy hopping) results in some exchange between *A* and *B* sites, we repeated the SEDOR experiment at an even lower temperature. The data at 104 K are quite similar to those at 145 K. The Gaussian decay curves corresponding to decay times of $T_2 = 377.4\ \mu$s and 513.7 μs corresponding to *A* and *B* beryllium atoms are also shown in Fig. 7 for comparison. These SEDOR results indicate that the two satellites *I* and *O* do not correspond to Be atoms *A* and *B* with two and one deuterium nearest neighbors, respectively.

D. Electronic calculations

For $ZrBe_2$ with no H ($x=0$), we find a charge transfer of about 0.64 electrons to each Be atom from the Zr atoms. For $x=2$ the charge transfer is 0.52 electrons to each Be atom and 0.25 electrons to each H, from the Zr atoms. These charges are determined by summing the charges on all orbitals centered upon the specific atom. This is a substantial charge transfer and suggests a considerable component of ionic bonding added to the metallic bonding. Further, the crystal structure suggests a sp^2 covalent bonding of Be that can be rationalized[15] if each Be has a formal charge of -1.

When increasing the number of H atoms in a supercell, the energy change per added H remains constant from $x=0$ to $x=1.38$, to within small variations in energy resulting from changes in the positions of the H atoms for fixed *x*. These variations are approximately 0.2 eV per supercell. At approximately $x=1.38$, the added energy per H atom starts to decrease gently. The decrease in total energy from a line with the constant initial slope (as a function of *x*) amounts to about 1 eV at $x=1.5$, increasing to about 6 eV at $x=2.0$. There is nothing remarkable about the changes in the density of states near $x=1.5$, the maximum H,D concentration obtainable with modest pressures. This suggests that $x=1.5$ is merely the value at which the free energy (a slowly varying function of *x*) for an additional H atom becomes greater than half the free energy of an externally placed H_2 molecule.

In order to shed light on the vacancy-ordered structure we have also investigated the energies of several distributions of H within a supercell at fixed *x*. For small *x* the energy is lowest when the H atoms are kept apart from each other; presumably this corresponds to the solid solution phase. When the fraction of vacancies is less than 0.5 ($x>1$) we find that the energy is lowest when the vacancies are kept apart. In both limits this quasiordering in the *ab* plane is more important energetically than the ordering in the *c* direction. The magnitude of energy change as a function of vacancy positions is about 0.2 eV for the supercells with 8 Zr and 16 Be. This is 0.008 eV/(total metal atom), which translates to a temperature of about 100 K. Although this is hardly a large effect, it is significant. This supports the finding by ^{9}Be NMR that the system undergoes a vacancy ordering at low temperatures.

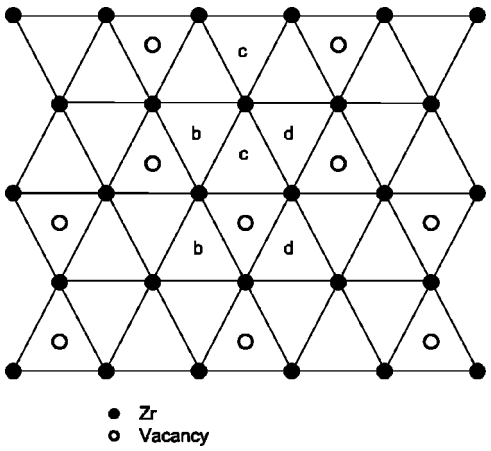

FIG. 8. Suggested in-plane structure of ordered hydrogenic vacancies. Filled circles are Zr atoms; H or D atoms (not shown) reside in the centers of Zr triangles. The vacancies shown by open circles are in location *a*; alternate (shifted) locations for neighboring planes are *b*,*c*,*d*.

We propose a structure for the vacancy ordering in Fig. 8 for $x=1.5$. This configuration has the lowest energy of any we attempted, though nearby (similar) configurations have only slightly greater energies. The configuration of Fig. 8 keeps the vacancies far apart. The stacking order (e.g., *acac* . . .) cannot be determined with the present level of accuracy, as the energy differences are too small.

IV. CONCLUSIONS

A temperature-induced transition in $ZrBe_2(H/D)_x$ has been studied by ^{9}Be NMR. The strong increase in ^{2}D T_2^{-1} observed previously signals a rapid decrease in the rate of D motion below T_c, demonstrating that the transition is an ordering of the D-atom vacancies (for $x \simeq 1.5$ as studied here, one-fourth of the D-atom sites are vacant). The ^{9}Be spectra show dramatic changes across narrow temperature intervals, revealing the presence of the transition in both hydride and deuteride at different temperatures (200 and 235 K, respectively). In both cases, above the transition temperature one pair of quadrupolar satellites occurs; below the transition each satellite splits into two resonances. The discontinuous temperature dependence of the quadrupolar splittings ν_Q and the appearence of two-phase coexistence in the spectra show the transitions to be first order. Electronic structure and energy calculations show a decreased H binding energy above $x=1.38$ and allow a vacancy-ordered structure to be proposed.

The two low-frequency ^{9}Be satellite resonances, inner and outer, show very similar ^{9}Be-^{2}D SEDOR dephasing curves, implying that the two ^{9}Be satellites arise from Be atoms with similar average D-atom environments. Thus, the SEDOR results are incompatible with the simplest interpretation of the ^{9}Be spectra, namely that one satellite is from Be atoms with two D-atom nearest neighbors (in the $\pm c$ direction) and the other satellite is from Be atoms with one D-atom neighbor and one D-vacancy neighbor. Instead, the SEDOR results indicate that both kinds of Be atoms, those

with one and two D neighbors, contribute approximately equally to the two satellite resonances, inner and outer. It appears that the EFG at a Be atom is less sensitive to the presence of a nearest-neighbor D-atom vacancy than to the location and presence of other vacancies. Indeed, each of the two satellites is quite broad, suggesting that the locations of several vacancies are important in determining the Be EFG. We note that the line shape of the satellites in the vacancy-ordered phase suggests that angular factors may be important; that is, the EFG is no longer uniaxially symmetric and/or the unique axis is no longer along the crystallite's *c* axis.

Beryllium NMR spectra demonstrate a surprisingly strong preferential alignment of the powder particles of $ZrBe_2(H/D)x$ due to magnetic susceptibility anisotropy and the high magnetic fields used for NMR, with the crystallites' *c* axes perpendicular to the applied magnetic field. A report of the magnetic alignment of powder $ZrBe_2(H,D)_x$ and other hexagonal metal deuterides has been prepared.[16]

ACKNOWLEDGMENTS

This research was supported by NSF Grant No. DMR-9987888. V.D.K. thanks Washington University, Department of Physics, and the Luthra family for support of travel. The research was partially supported by the Jet Propulsion Laboratory, California Institute of Technology, under a contract with the National Aeronautical and Space Administration. The work at Knox was supported by Research Corporation and NSF Grant No. DMR-9804094. We are grateful to Dr. A. J. Maeland for providing the samples used in these studies.

*Present address: Dept. of Radiology, UT Southwestern Medical Center at Dallas, 5323 Harry Hines Blvd., Dallas, Texas 75390.

[1] J. W. Nielsen and N. C. Baenziger, Acta Crystallogr. **7**, 132 (1954).
[2] A. J. Maeland and G. G. Libowitz, J. Less-Common Met. **89**, 197 (1983).
[3] A. F. Andresen, K. Ontes, and A. J. Maeland, J. Less-Common Met. **89**, 201 (1983).
[4] D. G. Westlake, Mater. Res. Bull. **18**, 1409 (1983).
[5] R. C. Bowman, Jr., D. R. Torgeson, and A. J. Maeland, Z. Phys. Chem. (Munich) **181**, 181 (1993).
[6] A. F. McDowell, C. F. Mendelsohn, M. S. Conradi, R. C. Bowman, Jr., and A. J. Maeland, Phys. Rev. B **51**, 6336 (1995).
[7] F. Kimmerle, G. Majer, U. Kaess, A. J. Maeland, M.S. Conradi, and A. F. McDowell, J. Alloys Compd. **264**, 63 (1998).
[8] B. C. Hauback, H. Fjellvåg, and A. J. Maeland, J. Alloys Compd. **224**, 241 (1995).
[9] V. Kodibagkar, J. L. Herberg, R. C. Bowman, Jr., and M. S. Conradi, J. Alloys Compd. **330-332**, 179 (2002).
[10] J. Haase, N. J. Curro, and C. P. Slichter, J. Magn. Reson. **135**, 273 (1998).
[11] M. Emshwiller, E. L. Hahn, and D. Kaplan, Phys. Rev. **118**, 414 (1960).
[12] C. P. Slichter, *Principles of Magnetic Resonance*, 3rd ed. (Springer, New York, 1990).
[13] A. Abragam, *Principles of Nuclear Magnetism* (Oxford University Press, Oxford, 1961).
[14] J. Korringa, Physica (Amsterdam) **15**, 601 (1950).
[15] Yue Wu (private communication).
[16] V. D. Kodibagkar, C. D. Browning, X. Tang, Y. Wu, R. C. Bowman, Jr., and M. S. Conradi (unpublished).